STUDY OF THE COMPLETE FUSION MECHANISM IN THE $^{16}O + ^{63}Cu$ REACTION

M. LANGEVIN, J. BARRETO and C. DETRAZ.

IPNO-PhN-76-06
FR7602841

STUDY OF THE COMPLETE FUSION MECHANISM IN THE $^{16}O+^{63}Cu$ REACTION

M. Langevin, J. Barreto* and C. Détraz

Institut de Physique Nucléaire, B.P. n°1, 91406 ORSAY, France

Abstract.

Absolute values of the cross sections for most evaporation channels consecutive to the complete $^{16}O+^{63}Cu$ fusion have been measured for incident ^{16}O energies ranging between 40 and 85 MeV, through the observation of the corresponding γ activities. They give evidence for a limitation in the contributing incident partial waves for energies above 50 MeV. The excitation functions of the various evaporation channels are satisfactorily accounted for, in shape and magnitude, by statistical evaporation calculations performed with the code ALICE. They allow a very precise determination of the variation of the critical angular momentum with the excitation energy of the compound nucleus.

NUCLEAR REACTIONS $^{63}Cu(^{16}O,X)$. E = 40-85 MeV
Measured E_γ , I_γ ; deduced $\sigma(X,E)$, critical angular momentum. Enriched target.

* Fellow of the Conselho Nacional de Desenvolvimento Ci·ntifico e Technologico, Brazil.

In the light of these results, a systematic study of the determination of ℓ_{cr} over a wide range of incident energies and for a medium-mass compound nucleus appears necessary to allow a reliable comparison with the many existing and sometimes conflicting theoretical predictions. The study of the complete fusion mechanism in the $^{16}O+^{63}Cu$ reaction which is reported in this paper[7] also aimed at testing the validity of the evaporation statistical model, which allows an estimation of the various de-excitation channels of the compound nucleus[8-11], in a case which is free of fission competition.

II - EXPERIMENTAL PROCEDURE

The cross section of complete fusion in the $^{16}O+^{63}Cu$ interaction has been measured for incident ^{16}O energies ranging between 40 and 85 MeV in 5 MeV steps. The ^{16}O beam was delivered by the Orsay MP Tandem. The ^{63}Cu targets were isotopically enriched to 99,76%. They were evaporated onto a thick gold backing (0.2 mm) which provided mechanical rigidity and collected the recoil nuclei. The thickness of the ^{63}Cu targets was measured by weighting with a 5% absolute error and ranged between 250 and 880 μg/cm^2.

The cross sections for the various (^{16}O,X) reactions were determined from the intensity of the γ-rays associated with the β decay of the residual nuclei. The γ-rays were measured by a 72 cm^3 Ge(Li) detector with an efficiency determined within 8% by use of calibrated γ sources.

For the observation of short-lived activities, the incident beam was mechanically chopped and four successive γ-ray spectra were recorded inbetween beam bursts. In the case of longer half-lives the target was manually transfered to a low-background area for recording of the γ-activity. In both cases, the residual nuclei were unambiguously identified through the energy and half-life of the γ-rays.

Table I summarizes the characteristics of the main γ-rays used in identifying the residual nuclei and measuring the corresponding cross sections.

The upper incident energy, 85 MeV, which is slightly above the Coulomb barrier for the $^{16}O+^{197}Au$ reaction, corresponds to the occurence of strong activities due to the target backing.

III - EXPERIMENTAL RESULTS

The 14 measured excitation functions for evaporation channels from the compound nucleus formed in the $^{16}O+^{63}Cu$ complete fusion appear in fig.1 to 5. Four reactions, i.e. (^{16}O,3pn), (^{16}O,αp), (^{16}O,α2p) and (^{16}O,αpn) could not be studied either because the residual nucleus was stable, or because a long half-life associated with a small cross section made the measurement of the corresponding γ-rays uncertain. The corresponding cross sections have been estimated from the experimental results for analog evaporation channels such as 3np, αn and α2n, and from the theoretical analysis of the excitation functions discussed below. These four cross sections contribute for less than 25% to the cross section for complete fusion. Therefore the latter one can be calculated to a good accuracy. Its variation with the incident energy is given in figure 6. The values of the observed cross sections between 40 and 50 MeV are in good overall agreement with the recent results of Wells et al.[12]. The experimental results of Natowitz[15] obtained at higher energy appear compatible with an extrapolation of those reported in this work and will be used in part of our analysis.

Yet the present results shed some light on disagreeing information published on the decay of ^{76}Rb. We have not observed the 181 keV γ-ray assigned to ^{76}Rb by Velandia et al.[13] and apparently observed by Wells et al.[12] but we confirm the assignment to ^{76}Rb made at Isolde[14] of four γ-rays of 344, 354, 424 and 885 keV energy with an observed half-life of 34±3 sec, in good agreement with the Isolde values.

IV - DISCUSSION AND CONCLUSIONS

A) Determination of the critical angular momenta

The excitation functions measured in this work were compared to the predictions of the statistical evaporation model, as calculated by the code ALICE[16] under two extreme assumptions : i) without taking into account the angular momentum of the compound nucleus[21] ; and ii) by assuming that the compound nucleus behaves like a rotating liquid drop with the contribution of all the incident partial waves. As seen in fig.1 to 5, the first assumption fails to account for the shapes and magnitudes of the measured cross sections. The second one though correctly predicts the magnitude of the maximum cross section for most evaporation channels. However its agreement with experimental results worsens with increasing incident energy. This indicates that high -ℓ partial waves do not contribute (or contribute less) to the formation of a compound nucleus.

Some of the evaporation channels being particularly sensitive to the contribution of higher-ℓ partial waves, the analysis of their excitation functions allows a precise determination of the largest contributing angular momentum, or ℓ_{cr}, as a function of incident energy. The uncertainty appears to be better than $\pm 1\hbar$, and the value of ℓ_{cr} determined in this way is remarkably identical for all the evaporation channels examined.

Such a determination depends upon the assumptions built into the code ALICE. It has to be checked by analyzing the total cross section for complete fusion, which is given by the relation[17]

$$\sigma_{CF} = \pi \lambda\!\!\!^{-2} \sum_{\ell=0}^{\ell_{cr}} (2\ell+1) \simeq \frac{\pi\hbar^2}{2\mu E_{CM}} \ell_{cr}^2$$

where μ is the reduced mass of the interacting nuclei.

An uncertainty of about 12% has been estimated for the experimental value of σ_{CF}. It is due, in particular, to uncertainties in the absolute efficiency of the Ge(Li) detector and in target thickness. Hence the determination of ℓ_{cr} from the values of σ_{CF} is rather dubious up to

50 MeV incident energy. Above 50 MeV it agrees with -but is somewhat less accurate than- the values derived from the analysis of particular evaporation channels, which will be used in the further analysis.

Table 2 summarizes the values of ℓ_{cr} determined by both methods, as well as the values ℓ_{gr} available in a grazing $^{16}O+^{63}Cu$ collision. Fig.7 represents the variation of ℓ_{cr} as a function of the excitation energy of the compound nucleus.

B) Validity of the predictions of the code ALICE

The truncation of the contributing partial waves at a maximum ℓ_{cr} value leads to an excellent overall agreement between the experimental excitation functions and the predictions of the statistical model computed with the code ALICE (fig.1 to 5).

The remaining disagreement results from an apparent underestimation of the evaporation probability of an α particle (fig.3) and from the correlated overestimation of 2pn and p2n evaporation at high incident energies. This effect is amplified for the evaporation of two α particles (fig.5). In this case, ALICE seems to grossly underestimate the cross sections, while the energy thresholds and shapes of excitation function remain rather correctly reproduced.

Rather than blaming the evaporation calculation for these disagreements, one could examine the possibility of contributions from direct reaction processes such as an $(^{16}O,^{8}Be)$ reaction possibly followed by the emission of unbound nucleons. However such a possibility appears unlikely in view of the modest cross section observed (fig.8) for the probably more abundant $(^{16}O,^{12}C)$ direct process.

C) The ^{73}Se isomeric ratio

Both the ground ($J^{\pi} = 7/2^{+}$, $T_{1/2} = 7.1h$) and isomeric ($J^{\pi} = 1/2^{-}$, $T_{1/2} = 39$ m) states of ^{73}Se were observed through their characteristic γ-activities.

The analysis of their respective excitation functions which are strikingly different (fig.4) has been made in the framework of the sharp-cutoff approximation[18,19]. This assumes that all the incident partial waves up to a value ℓ_f contribute to the formation of the lower-spin state, while higher-ℓ ones, above ℓ_f and up to ℓ_{cr}, lead to the population of the higher-spin state. At each incident energy, the ratio of the cross sections to the two states provided a value of ℓ_f from a partial-wave analysis given by the code ALICE. The variation of ℓ_f obtained by this procedure (fig.9) leads to a good agreement between the experimental and calculated cross sections. The value of ℓ_f for the maximum cross sections, at 65 MeV incident energy, is also in good agreement with the predicted value[19].

D) Analysis of the limitation of the complete fusion cross section

In section IV.A, the fact that σ_{CF} was smaller than the total cross section was assigned to a limitation in the contribution of higher-ℓ partial waves to the compound nucleus formation. The variation of σ_{CF} with incident energy was parametrized by use of a critical angular momentum ℓ_{cr} (table 2).

The assumption that the limitation of σ_{CF} is due to the dynamics of the entrance channel suggests another parametrization, in terms of a critical interaction radius r_{cr}, from another expression[20] of the complete fusion cross section.

$$\sigma_{CF} = \pi R_{cr}^2 (1 - V_{cr}/E_{CM}) .$$

with

$$R_{cr} = r_{cr}(A_1^{1/3} + A_2^{1/3})$$

Under the assumption[17,20] $V_{cr} = V_B$, where V_B is the Coulomb barrier in the entrance channel, measured in the center-of-mass system, $V_{cr} = V_B$ is equal to 32.9 MeV in the present case and values of r_{cr} can be deduced from the experimental results. They appear in table 2.

The experimental variation of r_{cr} with incident energy is shown in fig.10. Galin et al.[4] have suggested that r_{cr} is constant with energy and has a value of 1.00 ± 0.07 f. The results shown in fig.10 indicate that r_{cr} actually decreases with increasing energy. From a value close to the geometrical radius r_0 near the Coulomb barrier, it tends towards smaller values when E_{CM} exceeds 50 MeV.

From these various analysis, a limitation in the contribution of higher-ℓ partial waves is clearly documented. Its origin however cannot be readily established. A comparison between the experimental results and the available theoretical predictions is presented in fig.11. Quite obviously none of the theories satisfactorily reproduce the data. In particular no conclusion can be drawn as to the origin of the experimental limitation of σ_{CF}. Whether it is due to dynamic restrictions in the formation of the compound nucleus in the entrance channel, or to a structural limitation in the possible angular momenta of the compound nucleus itself will require more experiments. One possible test would be to study the variation of ℓ_{cr} with the excitation energy of the compound nucleus for different entrance channels.

Acknowledgments

The authors are indebted to Ms C. Cabot and Dr. F. Plasil for their collaboration in the use of the code ALICE. The assistance of Dr. F. Pougheon and Dr. J. Vernotte in taking some of the experimental data is gratefully acknowledged.

References

1) R. Bass, Phys. Lett. 47B (1973) 139.

2) J. Wilczynski, Nucl. Phys. A216 (1973) 386.

3) S. Cohen, F. Plasil and W.J. Swiatecki, Ann. Phys. 82 (1974) 557.

4) J. Galin, D. Guerreau, M. Lefort and X. Tarrago, Phys. Rev. C9 (1974) 1018.

5) M. Lefort, Y. Le Beyec and J. Péter, International Conference on Reactions Between Complex Nuclei, Nashville. USA), June 1974

6) M. Conjeaud, S. Harar, E.F. Da Silveira and C. Volant, Nucl. Phys. A250 (1975) 182.

7) A detailed report of the experimental method and results is given in J. Barreto, Thèse de 3ème cycle, IPN, Orsay (unpublished).

8) F.S. Stephens, J.R. Leigh and R.M. Diamond, Nucl. Phys. A170 (1971) 321.

9) J.R. Grover and J. Gilat, Phys. Rev. 157 (1967) 802 and Phys. Rev. C3 (1971) 734.

10) M. Blann, Phys. Rev. 157 (1967) 860.

11) M. Blann and F. Plasil, Phys. Rev. Lett. 29 (1972) 303.

12) J.C. Wells Jr., R.L. Robinson, H.J. Kim and J.L.C. Ford Jr, Phys. Rev. C5 (1975) 1529.

13) J.A. Velandia, W.I. Holmes and G.G.J. Boswell, J. Inorg. Nucl. Chem. 34 (1972) 401.

14) H.L. Ravn, S. Sundell, L. Westgaard and E. Roeckl, J. Inorg. Nucl. Chem. 37 (1975) 383 and private communication.

15) J.B. Natowitz, Phys. Rev. C1 (1970) 623.

16) M. Blann and F. Plasil, "Alice : a nuclear evaporation code", U.S. Atomic Energy Commission, Report n°COO-3494-10 (1973).

17) D. Glas and U. Mosel, Nucl. Phys. A237 (1975) 429.

18) J.M. Alexander and G.N. Simonoff, Phys. Rev. 130 (1963) 2383.

19) Y. Le Beyec, M. Lefort and M. Sarda, Nucl. Phys. A192 (1972) 405.

20) M. Lefort, "Critical discussion of the concept of critical angular momentum in heavy ion reactions", Rapport IPNO-RC-74-08. Orsay.

21) V.F. Weisskopf and D.H. Ewing, Phys. Rev. 57 (1940) 4[illegible].

22) E. Roeckl, D. Lode and W. Pessarra and the Isolde Collaboration, Z. Physik 265 (1974) 123.

Table 1. Characteristics of the γ-rays used in determining absolute cross sections for the $^{63}Cu(^{16}O,X)$ reactions.

X	Residual nucleus	E_γ (keV)	$T_{1/2}$	Branching ratio[a] (%)
2n	^{77}Rb	178.9	3.6 mn	38.4
pn	^{77}Kr	130.0	75.0 mn	87.3
p2n	^{76}Kr	315.7	14.6 h	36.0
p3n	^{75}Kr	132.7	4.5 mn	100.0
2p	^{77}Br	239.0	56.0 h	23.6
2pn	^{76}Br	559.2	16.0 h	77.0
α	^{75}Br	286.5	95.5 mn	75.0
αn	^{74}Br	634.6	38.0 mn	90.5
α2n	^{73}Br	669.5	3.3 mn	20.0
αpn	$^{73}Se^m$	253.8	39.0	4.0
αpn	$^{73}Se^g$	361.0	7.2 h	95.0
α2pn	^{72}As	834.0	26.0 h	80.0
2α	^{71}As	174.9	64.8 h	91.1
2αn	^{70}As	1040.0	53.0 mn	81.7
2αpn	^{69}Ge	1107.0	39.2 h	30.0

[a] The γ branching ratio are taken from Nuclear Data Tables, except for the $(^{16}O,p3n)$ channel[22].

Table 2. Experimental values of the critical angular momentum (ℓ_{cr}) and interaction radius (r_{cr}).

E_{lab} (MeV)	σ_{CF} (mb)	σ_R (mb)	σ_{CF}/σ_R	ℓ_{max}	ℓ_{cr} (1)	ℓ_{cr} (2)	r_{cr} (fm)
40	13.63±1.84	17.42	0.78±0.10	9	9	-	-
45	198.48±5.23	256.86	0.77±0.02	18	18	-	1.301±0.032
50	428.65±7.82	509.98	0.84±0.01	23	22	-	1.340±0.025
55	622.29±10.24	711.75	0.87±0.02	28	24	23	1.356±0.021
60	783.71±11.85	875.46	0.89±0.02	32	26	26	1.365±0.019
65	902.42±16.22	1010.43	0.89±0.01	35	28	29	1.357±0.023
70	924.30±15.06	1123.21	0.82±0.01	37	30	31	1.296±0.020
75	976.77±18.56	1218.53	0.80±0.02	40	32	33	1.268±0.023
80	846.90±14.03	1269.87	0.67±0.01	42	34	34	1.143±0.018
85	900.00±16.67	1369.90	0.65±0.02	43	36	35	1.143±0.020

The values of ℓ_{cr} are obtained (see sect.IV.A) from (1) a partial wave analysis of excitation functions by the code ALICE ; and (2) the experimental complete fusion cross section as compared to the total reaction cross section.

Figure captions

Fig.1. Absolute cross sections for xn and pxn evaporation channels from the $^{16}O+^{63}Cu$ reaction at ^{16}O incident energy E_L in the laboratory system. The solid line curves are drawn through the experimental points. The predictions obtained with the code ALICE under several assumptions (see section IV.A) are also represented : by a dotted line when the angular momentum of the compound nucleus is not taken into account[21] ; by a mixed line when a rotating liquid drop model is assumed for the compound nucleus with all partial waves contributing ; by a dashed line when contributing partial waves are restricted to $\ell \leqslant \ell_{cr}$.

Fig.2. Absolute cross sections for (^{16}O,2pxn) evaporation channels (see fig.1 caption).

Fig.3. Absolute cross sections for (^{16}O,αxn) and (^{16}O,α2pxn) evaporation channels (see fig.1 caption).

Fig.4. Absolute cross section for (^{16}O,αpn) evaporation channel. Full points correspond to the formation of the $J^{\pi} = 1/2^-$ ^{73}Se isomer, open points to the ^{73}Se $J^{\pi} = 7/2^+$ ground state and triangles to the sum of the two cross sections. Three solid lines are drawn through those points. The theoretical results calculated with the code ALICE,as described in the figure 1 caption, apply to the summed cross section.

Fig.5. Absolute cross section for (^{16}O,2αxn) evaporation channels (see fig.1 caption).

Fig.6. Experimental cross section for the complete $^{16}O+^{63}Cu$ fusion as a function of the incident ^{16}O energy in the laboratory system. The solid line is drawn through the experimental points and the dotted line is the calculated (see e.g. ref.[19]) total reaction cross section.

Fig.7. Variation with the excitation energy in the compound nucleus of the critical angular momentum ℓ_{cr} as deduced (see sect.IV.A) from the experimental cross sections obtained in this work (open points) and reported by Natowitz[15] (full points). Also represented are the available angular momentum ℓ_{gr} for a grazing $^{16}O+^{63}Cu$ interaction, the angular momentum of the compound nucleus in the rigid rotor model, and the $J_{cr} = 42\hbar$ limit predicted for the $^{16}O+^{63}Cu$ system by Wilczsynski[2].

Fig.8. Excitation function for the $(^{16}O,^{12}C)$ reaction. The solid line is drawn through the experimental points. The evaporation calculations with the code ALICE correspond to the mixed line (see fig.1 caption).

Fig.9. Analysis of the ^{73}Se isomeric ratio with the sharp cut-off approximation. In this diagram the angular momenta are plotted versus the ^{16}O incident energy. The solid line reproduces (from fig.7) the values of the critical angular momentum. The full points correspond to the cut-off ℓ_f value obtained (see sect.IV.C) from a partial wave analysis of the ^{73}Se cross sections with the code ALICE. The open points correspond to the predicted[19] values of ℓ_f.

Fig.10. Variation of the experimental values of the critical interaction radius r_{cr} with the ^{16}O incident energy. Full points correspond to the data from this work and open points are deduced from the experimental results of Natowitz[15].

Fig.11. Variation of the complete fusion cross section for $^{16}O+^{63}Cu$ plotted as $\sigma_{CF}/\pi \lambda\!\!\!^{-2}$ in $\hbar^2$ units as a function of the center-of-mass ^{16}O incident energy. The experimental values are from this work (full points) and Natowitz[15] (open points). Curve (1) corresponds to the calculated (see e.g. ref.[19]) total reaction cross section, curve (2) to the model of Bass[1], curve (3) to a constant $r_{cr} = 1$ f value[4] and curve (4) to the prediction of Wilczynski[2].

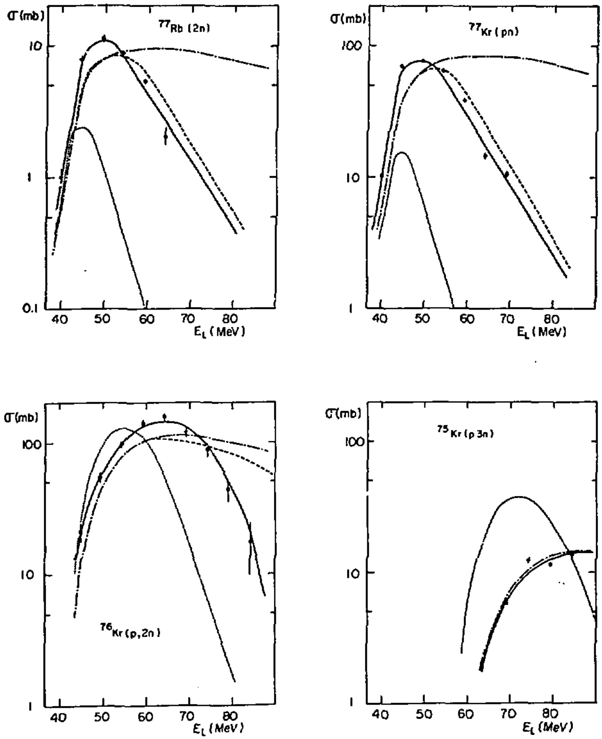

Fig.1

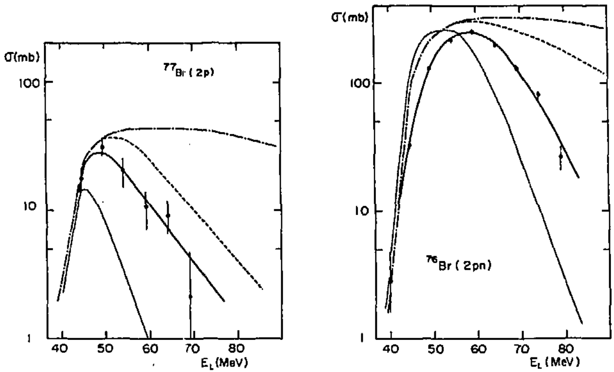
σ(mb)
100
10
1
^{77}Br (2p)
40
50
60
70
80
E$_L$ (MeV)
σ(mb)
100
10
1
^{76}Br (2pn)
40
50
60
70
80
E$_L$ (MeV)

Fig.2

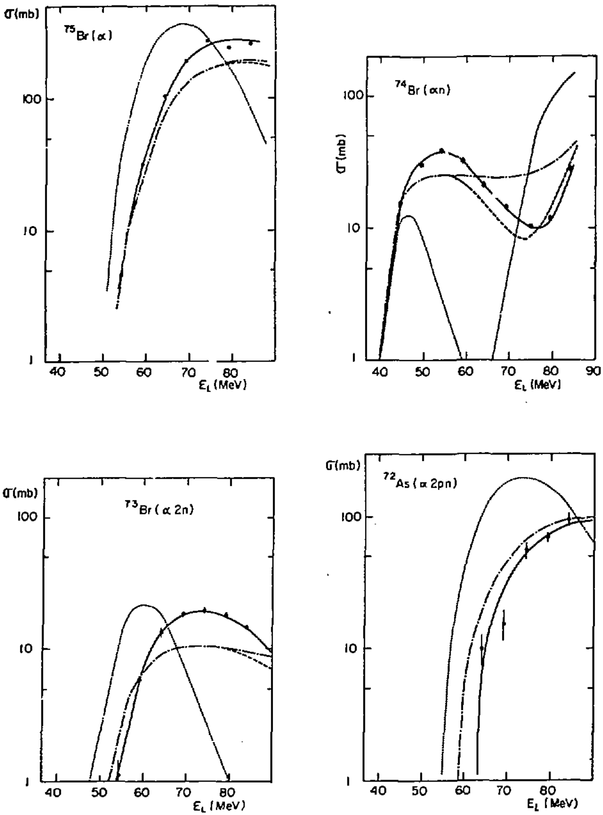
σ(mb)
^{75}Br (α)
100
10
1
40 50 60 70 80
E_L (MeV)
^{74}Br (αn)
σ(mb)
100
10
1
40 50 60 70 80 90
E_L (MeV)
σ(mb)
^{73}Br (α 2n)
100
10
1
40 50 60 70 80
E_L (MeV)
σ(mb)
^{72}As (α 2pn)
100
10
1
40 50 60 70 80
E_L (MeV)

Fig.3

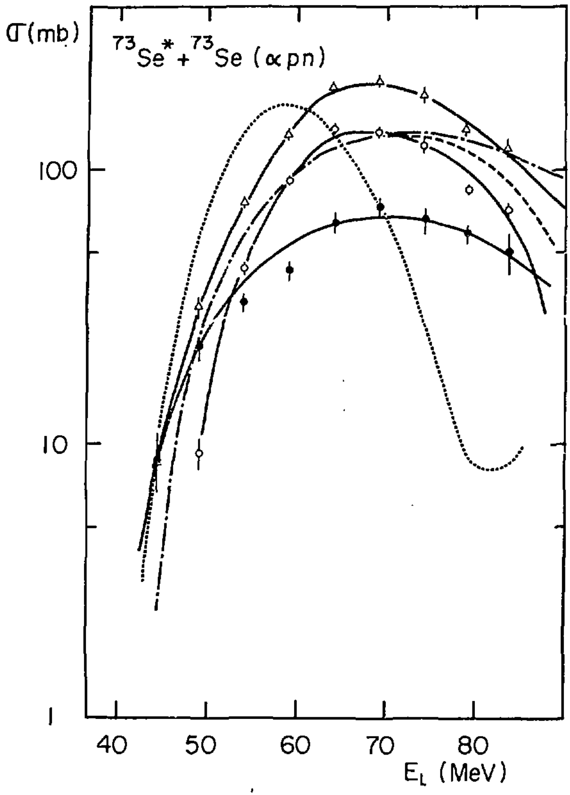

Fig.4

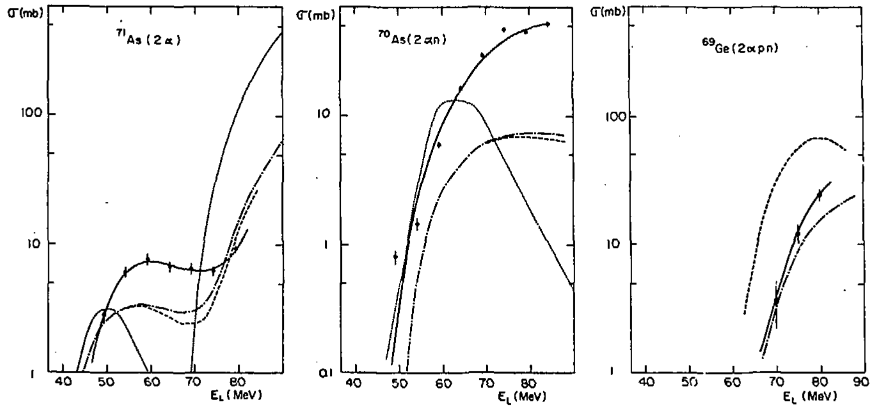
σ(mb)
^{71}As (2α)
100
10
1
40
50
60
70
80
E$_L$ (MeV)
σ(mb)
^{70}As(2αn)
10
1
0.1
40
50
60
70
80
E$_L$ (MeV)
σ(mb)
^{69}Ge(2αpn)
100
10
1
40
50
60
70
80
90
E$_L$ (MeV)

Fig.5

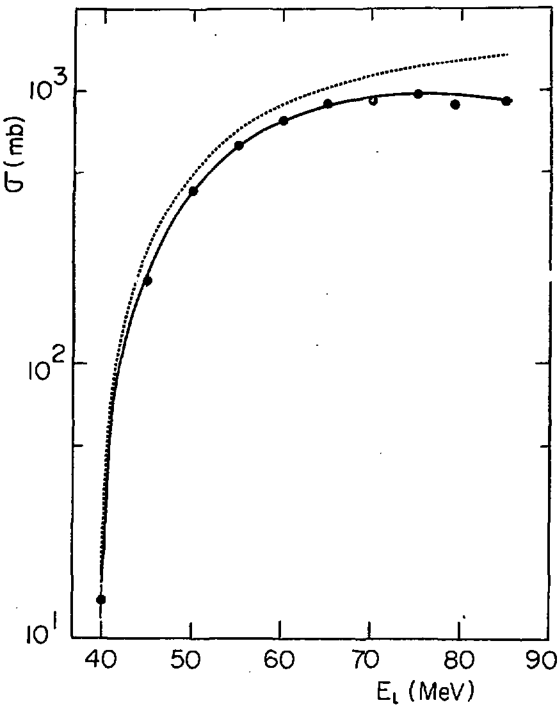

Fig.6

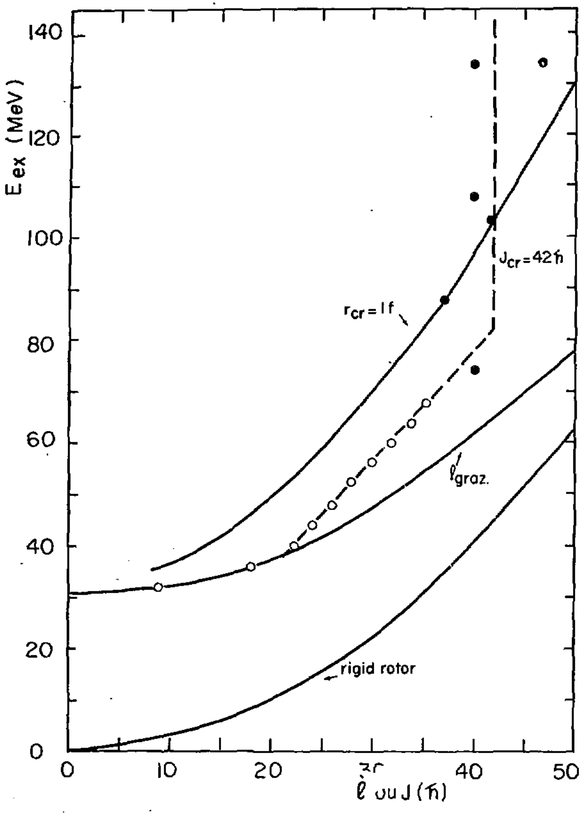
E ex (MeV)
140
120
100
80
60
40
20
0
0
10
20
40
50
ℓ ou J (ħ)
J cr = 42ħ
r cr = 1f
ℓ graz.
rigid rotor

Fig.7

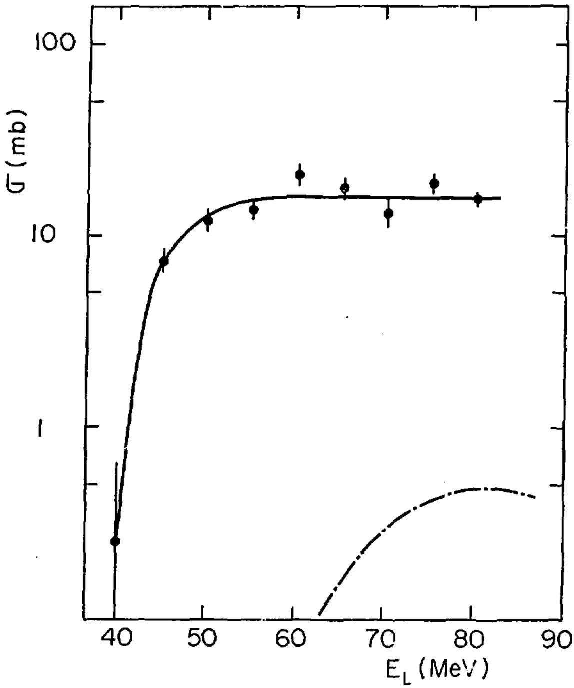

Fig.8

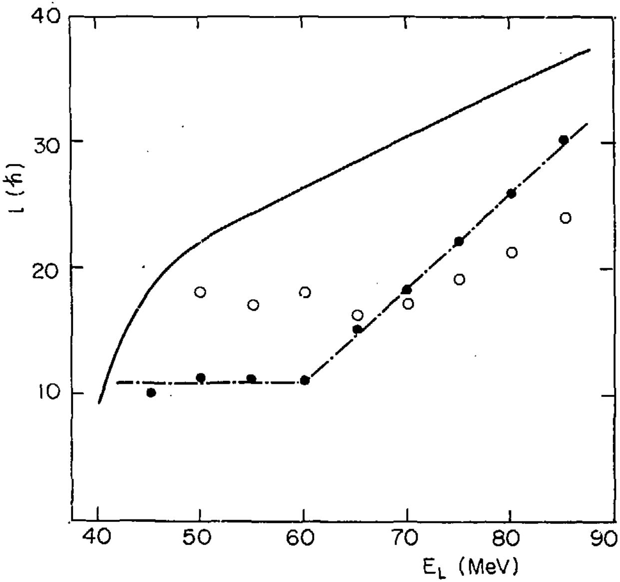

Fig.9

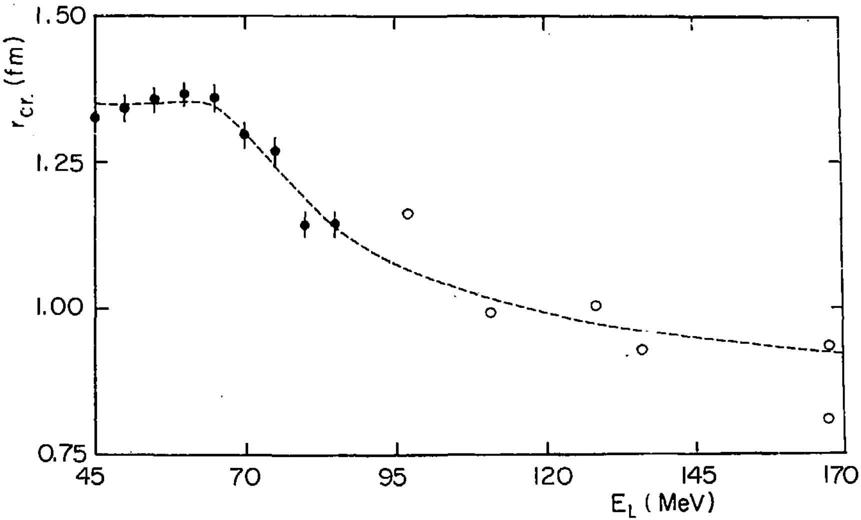

Fig.10

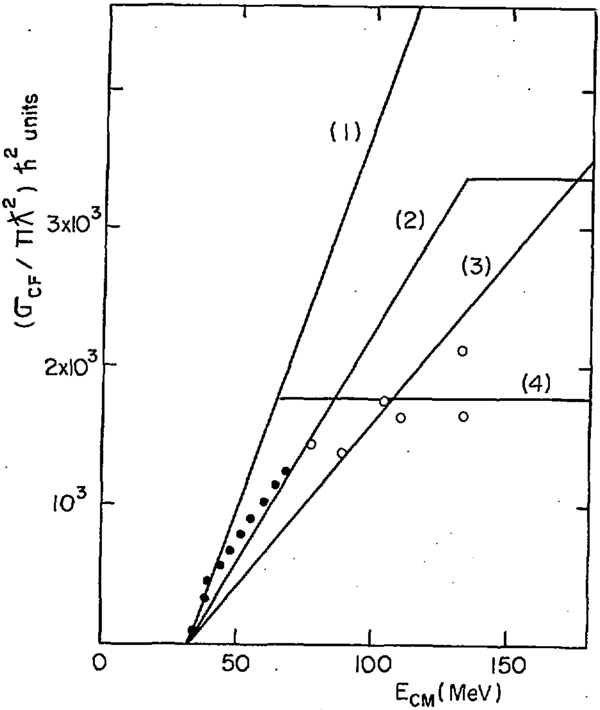

(1)
(2)
(3)
(4)
3x10^3
2x10^3
10^3
0
50
100
150
$(\sigma_{CF}/\pi\lambda^2)\ \hbar^2$ units
E_{CM} (MeV)

Fig. 11